cosmetics

MDPI

Article

Large Melanosome Complex Is Increased in Keratinocytes of Solar Lentigo

Kazuhisa Maeda [1,2]

[1] Bionics Program, Tokyo University of Technology Graduate School, 1404-1 Katakuramachi, Hachioji City, Tokyo 192-0982, Japan; kmaeda@stf.teu.ac.jp; Tel.: +81-426-372-442

[2] School of Bioscience and Biotechnology, Tokyo University of Technology, 1404-1 Katakuramachi, Hachioji City, Tokyo 192-0982, Japan

Received: 21 October 2017; Accepted: 7 November 2017; Published: 11 November 2017

Abstract: Solar lentigo (SL) is characterized by macular lesions exhibiting epidermal hyperplasia combined with hyperpigmentation along with irregular elongation of epidermal rete ridges. This study was conducted to assess the melanosomes in keratinocytes and the activation state of melanocytes in SL lesions on the backs of healthy Japanese individuals. Large melanosome complexes were increased in keratinocytes, and tyrosinase (TYR) activity, as well as immunohistochemical reactivity, for premelanosome protein 17 (Pmel17) in the SL lesions increased compared to the perilesions of five volunteers with SL. The levels of *TYR*, microphthalmia-associated transcription factor (*MITF*), and *KIT* mRNAs, but not stem cell factor (*SCF*) mRNA, were significantly increased in the SL lesions compared to the perilesions for all samples. Additionally, keratinocytes became immunoreactive to KIT in the rete ridge hyperplasia and basal layers of the SL lesions. These results suggested that the hyperpigmentation of SL arises primarily from increased melanogenesis of existing melanocytes in the basal layer of the epidermis, as well as increased large melanosome complexes in keratinocytes, which probably arise via an increase in KIT signaling in the epidermis.

Keywords: solar lentigo; melanosome; keratinocyte; melanocyte; KIT

1. Introduction

Solar lentigo (SL), also known as a sun-induced freckle or senile lentigo, is a hyperpigmentation that occurs increasingly with age in sun-exposed areas, such as the face, forearms, back, and the dorsal sides of hands. SL is a characteristic symptom of photoaged skin in contrast to ephelides [1]. Ephelides appear early in childhood and are associated with fair skin. Melanocortin-1 receptor (MC1R) gene variants are necessary to develop ephelides, although they are less important in the development of SL [2]. It is speculated that chronic exposure to UV radiation is a crucial pathogenic factor for the development of SL.

Many studies have been conducted on SL from both clinical and histological viewpoints. Miescher et al. proposed a clinical classification of SL involving three categories, including the small macular type, the large macular type, and the leukomelanoderma type [3]. In histological studies, Andersen et al. determined that 25 of 51 SL lesions on the face showed a flattened epidermis, 23 of 51 had a lentiginous epidermal hyperplasia, and three had a mixed flattened and lentiginous epidermal pattern [4]. These researchers further showed that facial SL had a statistically significant two-fold increase in both epidermal area and the number of melanocytes compared to facial skin with a similar degree of photodamage [4].

The number of dopa-positive melanocytes, or melanocytes that are immunoreactive with antibodies against melanogenic proteins, such as melanoma-associated antigen (Melan-A), tyrosinase (TYR), and tyrosinase-related protein-1 (TRP-1), also increased in SL lesions compared to the

perilesional areas [5–9]. Consequently, it has been assumed that the hyperpigmentation of SL might be due to an increase in the number of melanocytes in the basal layer of the epidermis. However, observations regarding the number of melanocytes are contradictory. Mehregan and Hölze observed no change in the number of melanocytes in relation to the length of the basal membrane [10,11], but other authors reported an increase [5–9,12]. Kadono et al. reported a two-fold increase in immunoreactive TYR-positive cells per length of the dermal/epidermal interface in the senile lentigo lesion compared to unaffected skin [7]. These researchers suggested that proliferation of melanocytes is increased in the senile lentigo epidermis. Cario-Andre et al. reported a significant increase (1.9-fold) in the number of Melan-A positive melanocytes per mm of the stratum corneum of senile lentigo, and melanocytes did not accumulate in the ridges, which is a finding that was confirmed by electron microscopy [8]. Noblesse et al. also reported a significant increase (2.1-fold) in the number of Melan-A positive melanocytes per mm of the stratum corneum in senile lentigo [9]. The discrepancies might be due to differences in the methods of skin preparation (e.g., split skin or sections), counting methods (e.g., dopa staining or immunostaining of melanogenic proteins), and how the area was measured (i.e., at the surface of the skin or at the basal layer of the epidermis).

However, it remains unclear whether the melanin deposition in the basal keratinocytes in the SL lesions is due to an increase in melanin synthesis in each melanocyte or due to an increase in the melanocyte population. In this study, we focus on the melanosomal complex in keratinocytes and the activation state of melanocytes in the epidermis of SL lesions, as well as perilesional normal skin biopsied from five volunteers. In the observations of the melanosome complex in keratinocytes made with transmission electron microscopy (TEM), we examined the number and the size of melanosome complexes in keratinocytes. We also evaluated immunochemical studies of the premelanosome protein 17 (Pmel17), which is required for the formation of the fibrillar compartment in the melanosome biogenesis that is critical to pigmentation [13], and KIT, which is expressed primarily in melanocytes and transformed epithelial tissues [14,15]. Additionally, we semi-quantitatively measured the gene expression of melanogenic proteins and related molecules.

2. Materials and Methods

2.1. Biopsies of SL Lesional and Perilesional Skin

Biopsy samples of SL lesional and perilesional normal skin from the back were obtained with a 3-mm punch from volunteers (n = 5; Japanese men) who ranged in age from 31 to 47 years (average, 40 years old). None of the subjects had hereditary factors that disposed them to ephelides, and all had a history of sun exposure on their back during their youth. All lesions were diagnosed as SL based on dermatoscopic criteria and using a DermLite II pro (3Gen, Dana Point, CA, USA). Skin was removed surgically from the upper dermis, and the samples were embedded in Tissue-Tek OCT compound (Sakura Finetechnical, Tokyo, Japan), snap-frozen with dry ice, and stored at −80 °C until use. All volunteers had given their informed consent to participate, and the study protocol was approved by the ethics committee.

2.2. Observations of Melanosomes in Keratinocytes Using Transmission Electron Microscopy (TEM)

The cultured cells were placed in 1.5% paraformaldehyde and 0.5% glutaraldehyde in phosphate buffered solution (PBS) at 4 °C for 1 h. After fixation, the specimens were washed in PBS, centrifuged, post-fixed in 1% osmium tetroxide, and centrifuged again, and the specimens were solidified in agar, which was finely sectioned. The samples were later dehydrated through an alcohol series and embedded in Epon epoxy resin to prepare blocks for electron microscopy. Toluidine-blue-stained specimens were prepared. After examination, one block per sample was selected for thin sectioning. The sections were examined using TEM (JEM-140, JEOL Ltd., Tokyo, Japan), and images were taken. The number and size of melanosomes per cell were measured by WinLoof (Mitani Corporation; Tokyo, Japan).

2.3. Tyramide-Based TYR Assay

TYR activity in cryostat sections (8 μm thick) was assayed according to the methods of Han et al. [16]. The sections were immediately air-dried then washed with phosphate-buffered saline (PBS), and incubated with a blocking buffer (10% goat serum) for 60 min at room temperature. Tetramethyl-tyramide, which was reconstituted in dimethyl sulfoxide according to the manufacturer's instructions (PerkinElmer, Winter Street Waltham, MA, USA), was diluted 150 times in amplification diluent and applied to the sections. The sections were incubated for 30 min at 37 °C, washed again with PBS, air-dried, and mounted with PermaFluor aqueous mounting medium (Thermo Shandon, Pittsburgh, PA, USA).

2.4. Immunohistochemistry

Cryostat sections (8 μm thick) were air-dried, fixed in cold acetone, washed with PBS, and incubated with the blocking buffer for 60 min at room temperature. Next, the sections were incubated for 60 min at room temperature or overnight at 4 °C in PBS with an antibody against KIT (K963, which is specifically reactive to the C-terminus of c-KIT, 1:150, IBL, Gunma, Japan) and Pmel17 (NKI-beteb; 1:10, Monosan, Uden, The Netherlands). After further washing in PBS, the sections were incubated for 60 min at room temperature with fluorescein-conjugated goat $F(ab')_2$ anti-mouse IgG (1:40, Biosource, Camarillo, CA, USA) or fluorescein-conjugated goat $F(ab')_2$ anti-rabbit IgG (1:40, Biosource). After further washing in PBS, the sections were air-dried and mounted with aqueous mounting medium.

2.5. Semi-Quantitative mRNA Analyses

Total RNA was extracted with an RNeasy Micro Kit (QIAGEN, Venlo, The Netherlands) from sections of the SL lesional and perilesional skin. Total RNA in each extract was quantified and its purity was assessed by spectrophotometry using an ND-1000 Spectrophotometer (Nanodrop Technologies, Wilmington, DE, USA). To synthesize the first-strand cDNA, a solution containing 50 ng of total RNA as the template, 1 μL of oligo dT (50 μmol/L) and 2 μL of 10 mmol/L dNTP was incubated for 5 min at 65 °C and then quickly transferred onto ice for another 5 min. After addition of 4 μL of 5′ First Strand Buffer (Invitrogen, Carlsbad, CA, USA), 1 μL of 0.1 mol/L dithiothreitol, 40 U (in 1 μL) of RNase inhibitor (Takara, Shiga, Japan), and 1 μL of SuperScript II RNaseH reverse transcriptase, the reaction mixture was incubated for 90 min at 4 °C and then for 15 min at 70 °C. PCR was performed using a Light Cycler RNA amplification kit with SYBR Green II (Roche Diagnostics, Mannheim, Germany). Primers for glyceraldehyde-3-phosphate dehydrogenase (*GAPDH*) were 5′-TGAACGGGAAGCTCACTGG-3′ and 5′-TCCACCACCCTGTTGCTGTA-3′. Primers for *TYR* were 5′-CCATGCATTTGTTGACAGT-3′ and 5′-TGTAGGATTCCCGGTTATGT-3′. Primers for microphthalmia-associated transcription factor, isoform M (*MITF-m*) were 5′-CTTAAAAGCATCCGTGGACT-3′ and 5′-AGACCCGTGGATGGAATAAG-3′. Primers for *KIT* were 5′-CACCTGCTGAAATGTATGAC-3′ and 5′-GACAGAATTGATCCGGAC -3′. Primers for *BCL-2* were 5′-TCATGTGTGTGGAGAGCG-3′ and 5′-GCCGTACAGTTCCACAAA-3′. Primers for stem cell factor (*SCF*) were 5′-CCATTTATGTTACCCCCTGT-3′ and 5′-GAGAAAACAATGCTGGCAAT-3′. After incubation at 95 °C for 10 min, Light Cycler PCR was performed for 40 cycles under the following conditions: (GAPDH) 95 °C for 15 s, 62 °C for 10 s, and 72 °C for 12 s; (*TYR*, *MITF-m*, *KIT*, *BCL-2*) 95 °C for 15 s, 55 °C for 10 s, and 72 °C for 12 s; (*SCF*) 95 °C for 15 s, 58 °C for 10 s, and 72 °C for 12 s. Each PCR reaction was performed in a total volume of 20 μL containing diluted cDNA template, forward and reverse primers (each at a final concentration of 0.5 μmol/L), and SYBR Green I master mix, including Taq DNA polymerase, reaction buffer, and a dNTP mix. Data were normalized to *GAPDH* levels and divided by the respective normalized values of the perilesional samples.

2.6. Enhanced Immunostaining of KIT in the Skin

Enhanced immunostaining of KIT was performed with a TSA fluorescence system (PerkinElmer). Briefly, cryostat sections (8 μm thick) were air-dried, fixed in cold acetone, washed with PBS, and incubated with 1% hydroperoxide for 30 min, then incubated in blocking buffer for 60 min at room temperature. The sections were further incubated overnight at 4 °C with an anti-KIT antibody (K963; 1:150, diluted in blocking buffer). After further washing with 0.05% Tween 20 in PBS, the sections were incubated with horseradish peroxidase-conjugated goat anti-rat IgG (1:200, diluted in blocking buffer, Biosource) in PBS for 60 min at room temperature. Next, after further washing in 0.05% Tween 20 in PBS, fluorescein-labeled tyramide was applied according to the manufacturer's protocol. The sections were air-dried and mounted with aqueous mounting medium.

2.7. Statistical Analysis

Measured values were analyzed for significant differences using an unpaired *t*-test (two-tailed) or a paired *t*-test (two-tailed) in Microsoft Excel (Microsoft, Redmond, WA, USA), and $p < 0.05$ was considered to be statistically significant.

3. Results

3.1. Microscopic and Histological Observations

Representative samples of SL are shown in Figure 1. All biopsy samples of SL were confirmed by microscopy to contain well-developed pigmented rete ridges. Histological observation of frozen sections showed that melanin was markedly deposited in the basal and, to a lesser extent, suprabasal layers of the epidermis in the SL lesional skin compared to the perilesional normal skin. Melanin was also occasionally apparent in the upper dermis of the SL lesions, whereas no melanin deposition was observed in the perilesional dermis. The dermal-epidermal junction in the SL lesions had many elongated epidermal rete ridges (Figure 1).

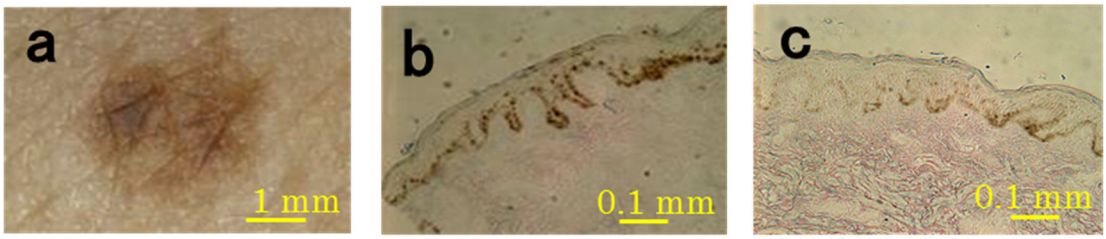

Figure 1. Representative microscopic features of SL lesions and perilesional normal skin (subject #4). The SL lesions were imaged with a video microscope (**a**) and sections were imaged with a light microscope ((**b**) SL lesion; (**c**) perilesion).

3.2. TEM Observations

The picture of the keratinocytes of the basal layer taken by TEM are shown in Figure 2. It was observed in all samples that the size of the melanosome complex of the SL lesion is larger than the perilesion (Figure 2). As a result of measuring the number and the size of melanosome complexes per cell, there were no significant differences in the number of melanosome complexes between SL lesion and perilesion samples (Figure 2). However, concerning the size of the melanosome complex, in the SL lesion was larger than in the perilesion in all samples, and a statistically significant difference was observed (Figure 2).

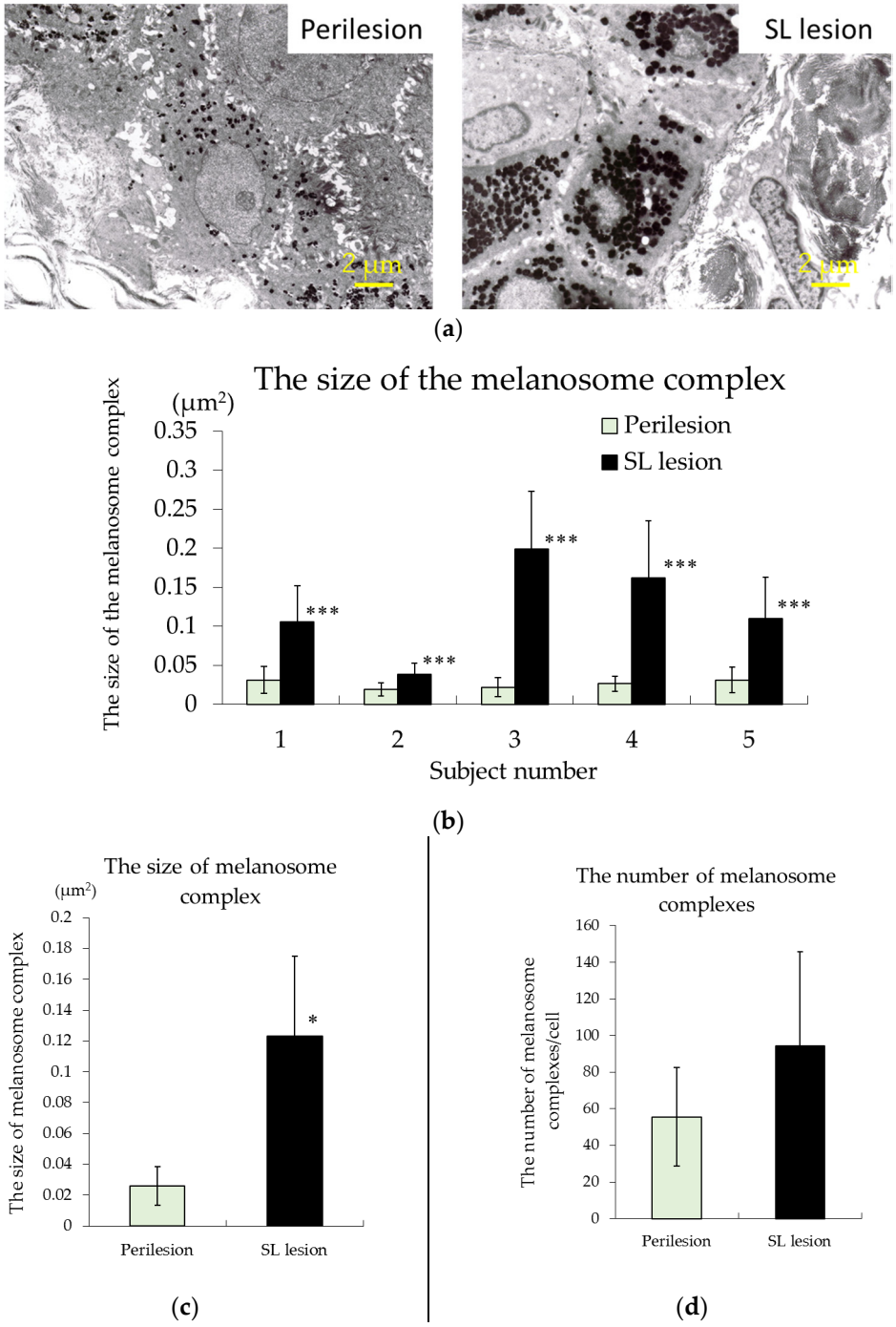

Figure 2. Representative electron micrographs (2700×) of biopsy samples of SL lesion and perilesional normal skin ((**a**), subject #4). The size of the melanosome complex ((**b**), individual; (**c**), mean) and the number of melanosome complexes ((**d**), mean) in the keratinocytes of the basal layer of the epidermis in the perilesion and SL lesion samples. The results are expressed as the mean ± standard deviation of five subjects. *** $p < 0.001$ vs. the perilesion of each subject by a paired *t*-test, * $p < 0.05$ vs. the perilesion according to an unpaired *t*-test.

3.3. TYR Activity of Melanocytes

The detection of TYR in melanocytes using a tyramide-based TYR assay of the skin sections was confirmed by double-staining with an anti-TRP-1 antibody. The number of TYR-positive melanocytes

increased in the basal layer of the SL lesional epidermis compared to the perilesion samples (Figure 3). No positive cells were seen in the upper dermis in either lesion (Figure 3). TYR activity in the SL lesion was increased compared to that in the perilesion in all samples.

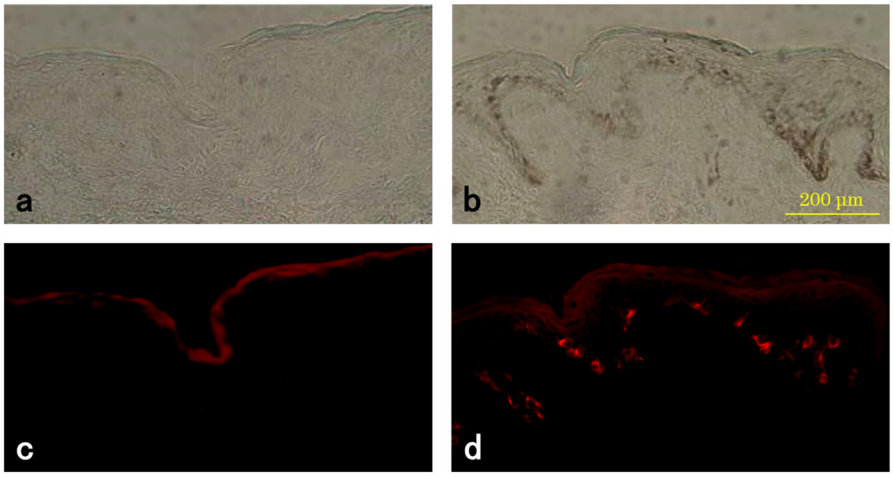

Figure 3. Histochemical measurement of tyrosinase (TYR) activity in SL lesions and perilesional normal skin. Representative sections of perilesional skin (**a**,**c**) and SL lesional (**b**,**d**) skin from the same subject (#2) were incubated with tyramide derivatives and photographed under a light microscope (**a**,**b**) or a fluorescence microscope (**c**,**d**). TYR-positive cells (stained red) are located on the basal layer. The weak staining of the stratum corneum appeared to be non-specific.

3.4. Level of Pmel17 in Melanocytes

Next, we examined the protein expression level of Pmel17, which is required for the formation of the fibrillar compartment in melanosome biogenesis, which is a process that is critical to pigmentation [17]. As shown in Figure 4, the Pmel17 immunopositivity was markedly increased, and the number of positive cells was greatly increased in the SL lesion compared to the perilesion. The Pmel17-positive melanocytes in the SL lesion were large and dendritic. Immunoreactive PMEL17 in the SL lesion was increased compared to that in the perilesion in all samples.

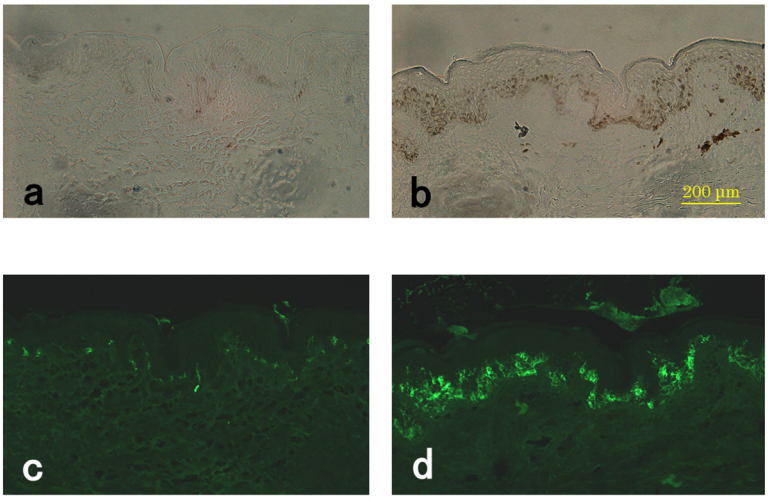

Figure 4. Expression of PMEL17 in the SL lesion and perilesional normal skin. Representative sections of perilesional (**a**,**c**) and SL lesional (**b**,**d**) skin from the same subject (#5). Light microscope images (**a**,**b**) and immunostaining of PMEL17 (**c**,**d**).

3.5. mRNA Levels of TYR, MITF-m, KIT, BCL-2, and SCF

MITF-m is a transcription factor that acts on promoters in genes encoding many melanogenesis-related proteins, including TYR, TRP-1, TRP-2, and PMEL17 [18–21]. The phosphorylation of MITF-m by KIT signaling induces an increase in *TYR* mRNA, as well as mRNAs of other melanogenic proteins, including TRP-1, TRP-2, and PMEL17 [22]. Therefore, we measured the mRNA levels of *TYR*, *MITF-m*, *KIT*, *BCL-2*, and *SCF* in the SL lesion and perilesion by semi-quantitative mRNA analyses. BCL-2, which is an anti-apoptotic protein, co-localized with KIT-positive melanocytes throughout the epithelium [23]. The BCL-2 expression was measured as a control because it was only expressed in melanocytes in the epidermis. As shown in Table 1, the levels of *TYR* and *KIT* mRNAs in the SL lesion were markedly increased by 5-, 8.2-, and 3.5-fold, respectively, compared to the perilesion in all samples. *KIT* mRNA increased in the SL lesion even when the epidermis was separated from the dermis. However, there was no difference in *BCL-2*, which is expressed in melanocytes in the epidermis between the SL lesion and perilesion. The level of *MITF-m* mRNA in the SL lesion was also significantly increased in four out of five samples (2.5-fold). For *SCF* mRNA, it was increased in the SL lesion in three out of five samples, but decreased in the other two, although the average increase was still 1.6-fold.

Table 1. Comparison of the relative expression of *TYR*, *MITF-m*, *KIT BCL-2*, and *SCF* mRNAs in SL lesion and perilesion samples.

mRNA	Relative Expression of mRNA	
	Perilesion	**SL Lesion (Mean ± Standard Deviation)**
TYR	1.0	4.9 ± 2.1
MITF-m	1.0	2.5 ± 1.4
KIT	1.0	3.6 ± 0.9
BCL-2	1.0	1.0 ± 0.5
SCF	1.0	1.7 ± 1.2

3.6. Enhanced Immunostaining of KIT in the Skin

Since *KIT* mRNA was markedly increased in the epidermis of the SL lesions, we used enhanced immunostaining to examine KIT antigens. The epidermal keratinocytes in the rete ridge hyperplasia and all the cells in the basal layer of all SL lesions were immunoreactive for KIT in addition to showing the high immunoreactivity of epidermal melanocytes (Figure 5). Immunoreactive KIT in the SL lesion was increased compared to that in the perilesion in all samples.

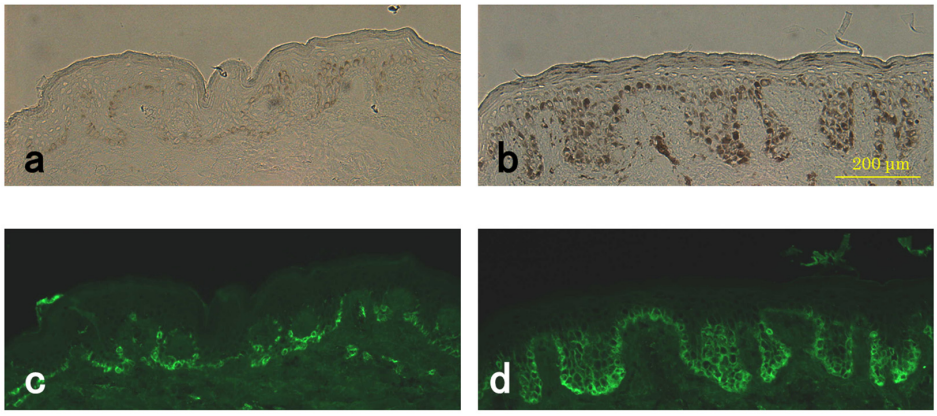

Figure 5. Detection of KIT in the SL lesion and perilesional normal skin using enhanced immunostaining methods. Representative sections of perilesional (**a**,**c**) and SL lesional (**b**,**d**) skin from the same subject (#4). Light microscope images (**a**,**b**) and immunostaining with KIT (**c**,**d**).

4. Discussion

Many reports have been produced on clinical, histological and molecular biology examinations of SL. Most authors agree that there is an increase of melanin in the basal layer of the epidermis with irregular elongation of epidermal rete ridges, as well as an increase in large melanosome complexes in basal keratinocytes of the epidermis [4–6,8–10]. The most characteristic and consistent finding is increased thickening of the epidermis with hypergranulosis, hyperkeratosis and proliferation of basaloid cells showing a marked increase in pigmentation, as well as forming buds and strands connected to the lower surface of the epidermis [10]. The histological observations of SL by light and electron microscopy in our study generally correlated with these previous findings. Large melanosome complexes were observed in basal keratinocytes in SL lesional skin. Noblesse et al. also reported a significant increase (2.1-fold) in the number of Melan-A positive melanocytes per mm of the stratum corneum and numerous melanosome complexes called polymelanosomes, which formed massive caps on the nuclei in basal keratinocytes of senile lentigo [9]. The immunological staining data indicated that the hyperpigmentation in the SL lesional skin was primarily observed because of the activation of melanocytes, i.e., inactive melanocytes residing in the SL lesion become activated, and this outcome is consistent with the increased level of TYR in cells in the SL lesion. Furthermore, Pmel17-positive melanocytes were markedly increased in the SL lesion, which reflects stimulation of melanosome biogenesis, as well as melanin synthesis in melanocytes in the SL lesions. We also observed an increase in cell size and elongation of dendrites of melanocytes in the SL lesion. These morphological changes of melanocytes are consistent with increased melanization due to the differentiation of melanocytes in the SL lesions. The melanosome complexes in keratinocytes are digested by lysosomal enzymes in the process of cornification, and most melanosomes are decomposed by formation of a stratum corneocyte [24–26]. If the diameter of a melanosome complex decreases than 400 nm, it will not be observed optically. Since the diameters of the melanosome complex of SL lesions are 305–464 nm, they can be observed visually, but since the diameters of the melanosome complex of perilesions are 139–223 nm, they are not detected visually. The size of melanosomes in Asian skin was reported to be 13.6 $\pm$ 1.5 nm [27]. Since the small melanosomes the melanocyte made are contained in the melanosome complex, it is believed that a melanosome complex containing many melanosomes develops a larger size.

The proto-oncogene c-Kit encoding the transmembrane tyrosine kinase receptor KIT is required for normal hematopoiesis, melanogenesis and gametogenesis [28]. Upregulation of KIT tyrosine kinase is also important for epidermal pigmentation. The levels of *TYR* and *KIT* mRNAs in the SL lesion were significantly increased compared to the perilesion in all samples (4.9- and 3.6-fold, respectively). *MITF-m* mRNA in the SL lesion was increased in four out of five samples, whereas *SCF* mRNA did not increase in five samples. KIT signaling activates the MAP kinase which, in turn, phosphorylates the transcription factor MITF-m that acts on the promoters of genes encoding TYR at a consensus target serine. This phosphorylation upregulates MITF-m transactivation of the *TYR* gene promoter [19]. Therefore, it is reasonable to consider that the phosphorylation of MITF-m by KIT signaling, rather than the increase of *MITF-m* mRNA, in the SL lesion induces an increase in *TYR* mRNA. SCF binding to KIT leads to internalization of KIT into the cytoplasm to be digested [29], and this change might result in upregulation of *KIT* mRNA in the SL lesion. KIT signaling is essential for differentiation and maturation of melanocytes, and the SCF/KIT pathway plays a critical role in homeostasis of normal human melanocytes [30]. In the present study, the mRNA level of *KIT* in the SL lesion was significantly higher compared to the perilesion. Since KIT is commonly expressed in almost all melanocytes in the basal layer of the epidermis, these results suggest that the increase of *KIT* mRNA is due to increased expression of *KIT* mRNA per cell. This hypothesis was supported by the finding that there was no difference in the expression level of *BCL-2* mRNA between the SL lesion and perilesion.

Interestingly, the enhanced immunostaining of the KIT antigen revealed that the plasma membrane of keratinocytes in the epidermal rete ridge hyperplasia and all the cells in the basal layer in the SL lesion were reactive to the anti-KIT antibody in addition to the high immunoreactivity

of melanocytes. Epithelial cells immunoreactive to KIT appear in hair matrix keratinocytes during the later stages of hair follicle development in mice [31]. *Kit* mRNA expression was highest during the growth phase of the hair cycle and at the onset of catagen development when not only mast cells and melanocytes, but also hair bulb keratinocytes, expressed Kit [32]. Many epithelial tissues appear to express KIT only when they are transformed but have low malignancy [14,15], which might reflect a situation in which proliferation is stimulated, and differentiation is suppressed. These findings are consistent with the idea that the high expression of KIT is associated with epithelial hyperplasia in the rete ridges in addition to epidermal melanogenesis during SL development. Binding of SCF to KIT results in homodimerization, followed by the transactivation of its intracellular tyrosine kinase. KIT stimulation activates signaling pathways, including the MAPK, PI3K, and JAK/STAT pathways, for a wide array of cytokines and growth factors [33,34]. Another mechanism of the upregulation of KIT tyrosine kinase has been postulated as follows. It was shown that mutation in the juxtamembrane domain enhanced the stability of KIT spontaneous dimerization, which leads to ligand-independent phosphorylation [35]. Mutation in the juxtamembrane domain of the *KIT* gene in gastrointestinal stromal tumors (GISTs) resulted in abnormal hyperpigmentation in the perineum and urticaria pigmentosa [36–38]. It is possible that sustained KIT stimulation is involved in abnormal hyperpigmentation via an SCF-dependent or SCF-independent mechanism. However, in future studies, it must be examined whether SCF-independent activation of KIT is involved in SL.

Conversely, it has been reported that the epidermal membrane-bound SCF is over-expressed in senile lentigo at the mRNA level (3.9-fold) by immunoblotting (1.6-fold) and by immunohistochemical observation, whereas the *KIT* mRNA transcripts showed no significant difference in expression (average 1.16-fold, n = 6, not significant, age 63–66) between non-lesional and senile lentigo lesional skin [39]. These results suggested that the pathogenesis and molecular mechanism might be different between senile lentigo and SL or may be affected by aging (63–66 years old versus 31–47 years old) and the SL lesional sites (arm, leg and face versus back). SCF plays an essential role in the increased proliferation of melanocytes, as shown by the observation of hypermelanosis in Scf transgenic animals [40] and the finding that subcutaneous injection of Scf resulted in hyperplasia of melanocytes [41]. Electron micrographs demonstrated that the melanocyte population was increased at a local Scf injection site compared to the noninjected tissue [41]. These results show that a local increase in SCF induces melanocytic proliferation in tissue, similar to how melanocyte proliferation in culture was stimulated by adding exogenous SCF.

Although SCF mRNA levels in the SL lesion were not increased in all samples, KIT levels in the SL lesion were increased compared to those in the perilesion in all the samples evaluated in this study. Therefore, the overexpression of KIT in the epidermis should be more important than the induction of SCF in the pathogenesis of SL.

5. Conclusions

The hyperpigmentation of SL lesions primarily occurred due to the stimulation of melanogenesis in melanocytes in the basal layer of the epidermis in the SL lesion. Moreover, the size of melanosome complexes was larger in the keratinocytes of the epidermal basal layer of the SL lesion than in the perilesion in all five subjects. This increase in size probably occurred due to an increase in KIT signaling in the epidermis rather than an increase in the number of melanosomes in keratinocytes and in the population of melanocytes.

Acknowledgments: The author gratefully appreciates Jun Matsunaga, who performed the biopsies to collect SL lesional and perilesional skin.

Conflicts of Interest: The author declares no conflicts of interest.

References

1. Bastiaens, M.; Hoefnagel, J.; Westendorp, R.; Vermeer, B.J.; Bouwes Bavinck, J.N. Solar lentigines are strongly related to sun exposure in contrast to ephelides. *Pigment Cell Res.* **2004**, *17*, 225–229. [CrossRef] [PubMed]
2. Bastiaens, M.; ter Huurne, J.; Gruis, N.; Bergman, W.; Westendorp, R.; Vermeer, B.J.; Bavinck, J.N.B. The melanocortin-1-receptor gene is the major freckle gene. *Hum. Mol. Genet.* **2001**, *10*, 1701–1708. [CrossRef] [PubMed]
3. Miescher, G.; Haberlin, L.; Guggenheim, L. Uber fleckformige Alterspingmentierungen: Ihre Beziehungen zur melanotischen pracancerose und zur senilen Warze. *Arch. Dermatol. Syph.* **1936**, *174*, 105–125. [CrossRef]
4. Andersen, W.K.; Labadie, R.R.; Bhawan, J. Histopathology of solar lentigines of the face: A semi-quantitative study. *J. Am. Acad. Dermatol.* **1997**, *36*, 444–447. [CrossRef]
5. Hodgson, C. Senile lentigo. *Arch. Dermatol.* **1968**, *87*, 197–207. [CrossRef]
6. Montagna, W.; Hu, F.; Carlisle, K. A reinvestigation of solar lentigines. *Arch. Dermatol.* **1980**, *116*, 1151–1154. [CrossRef] [PubMed]
7. Kadono, S.; Manaka, I.; Kawashima, M.; Kobayashi, T.; Imokawa, G. The role of the epidermal endothelin cascade in the hyperpigmentation mechanism of lentigo senilis. *J. Investig. Dermatol.* **2001**, *116*, 571–577. [CrossRef] [PubMed]
8. Cario-Andre, M.; Lepreux, S.; Pain, C.; Nizard, C.; Noblesse, E.; Taieb, A. Perilesional vs. lesional skin changes in senile lentigo. *J. Cutan. Pathol.* **2004**, *31*, 441–447. [CrossRef] [PubMed]
9. Noblesse, E.; Nizard, C.; Cario-Andre, M.; Lepreux, S.; Pain, C.; Schnebert, S.; Taïeb, A.; Kurfurst, R. Skin ultrastructure in senile lentigo. *Skin Pharmacol. Physiol.* **2006**, *19*, 95–100. [CrossRef] [PubMed]
10. Mehregan, A.H. Lentigo senilis and its evolutions. *J. Investig. Dermatol.* **1975**, *65*, 429–433. [CrossRef] [PubMed]
11. Hölzle, E. Pigmented lesions as a sign of photodamage. *Br. J. Dermatol.* **1992**, *127* (Suppl. 41), 48–50. [CrossRef] [PubMed]
12. Nakagawa, H.; Rhodes, A.R.; Momtaz-T, K.; Fitzpatrick, T.B. Morphologic alterations of epidermal melanocytes and melanosomes in PUVA lentigines: A comparative ultrastructural investigation of lentigines induced by PUVA and sunlight. *J. Investig. Dermatol.* **1984**, *82*, 101–107. [CrossRef] [PubMed]
13. Berson, J.F.; Harper, D.C.; Tenza, D.; Raposo, G.; Marks, M.S. Pmel17 initiates premelanosome morphogenesis within multivesicular bodies. *Mol. Biol. Cell* **2001**, *12*, 3451–3464. [CrossRef] [PubMed]
14. Tsuura, Y.; Hiraki, H.; Watanabe, K.; Igarashi, S.; Shimamura, K.; Fukuda, T.; Suzuki, T.; Seito, T. Preferential localization of c-kit product in tissue mast cells, basal cells of skin, epithelial cells of breast, small cell lung carcinoma and seminoma/dysgerminoma in human: Immunohistochemical study on formalin-fixed, paraffin-embedded tissues. *Virchows Arch.* **1994**, *424*, 135–141. [CrossRef] [PubMed]
15. Simak, R.; Capodieci, P.; Cohen, D.W.; Fair, W.R.; Scher, H.; Melamed, J.; Drobnjak, M.; Heston, W.D.; Stix, U.; Steiner, G.; et al. Expression of c-kit and kit-ligand in benign and malignant prostatic tissues. *Histol. Histopathol.* **2000**, *15*, 365–374. [PubMed]
16. Han, R.; Baden, H.P.; Brissette, J.L.; Weiner, L. Redefining the skin's pigmentary system with a novel tyrosinase assay. *Pigment Cell Res.* **2002**, *15*, 290–297. [CrossRef] [PubMed]
17. Hoashi, T.; Muller, J.; Vieira, W.D.; Rouzaud, F.; Kikuchi, K.; Tamaki, K.; Hearing, V.J. The repeat domain of the melanosomal matrix protein PMEL17/GP100 is required for the formation of organellar fibers. *J. Biol. Chem.* **2006**, *281*, 21198–21208. [CrossRef] [PubMed]
18. Tachibana, M.; Takeda, K.; Nobukuni, Y.; Urabe, K.; Long, J.E.; Meyers, K.A.; Aaronson, S.A.; Miki, T. Ectopic expression of MITF, a gene for Waardenburg syndrome type 2, converts fibroblasts to cells with melanocyte characteristics. *Nat. Genet.* **1996**, *14*, 50–54. [CrossRef] [PubMed]
19. Yasumoto, K.; Yokoyama, K.; Takahashi, K.; Tomita, Y.; Shibahara, S. Functional analysis of microphthalmia-associated transcription factor in pigment cell-specific transcription of the human tyrosinase family genes. *J. Biol. Chem.* **1997**, *272*, 503–509. [CrossRef] [PubMed]
20. Udono, T.; Yasumoto, K.; Takeda, K.; Amae, S.; Watanabe, K.; Saito, H.; Fuse, N.; Tachibana, M.; Takahashi, K.; Tamai, M.; et al. Structural organization of the human microphthalmia-associated transcription factor gene containing four alternative promoters. *Biochim. Biophys. Acta* **2000**, *1491*, 205–219. [CrossRef]

21. Du, J.; Miller, A.J.; Widlund, H.R.; Horstmann, M.A.; Ramaswamy, S.; Fisher, D.E. MLANA/MART1 and SILV/PMEL17/GP100 are transcriptionally regulated by MITF in melanocytes and melanoma. *Am. J. Pathol.* **2003**, *163*, 333–343. [CrossRef]
22. Hemesath, T.J.; Price, E.R.; Takemoto, C.; Badalian, T.; Fisher, D.E. MAP kinase links the transcription factor Microphthalmia to c-Kit signalling in melanocytes. *Nature* **1998**, *391*, 298–301. [PubMed]
23. Grichnik, J.M.; Ali, W.N.; Burch, J.A.; Byers, J.D.; Garcia, C.A.; Clark, R.E.; Shea, C.R. KIT expression reveals a population of precursor melanocytes in human skin. *J. Investig. Dermatol.* **1996**, *106*, 967–971. [CrossRef] [PubMed]
24. Otaki, N.; Seiji, M. Degradation of melanosomes by lysosomes. *J. Investig. Dermatol.* **1971**, *57*, 1–5. [CrossRef] [PubMed]
25. Ebanks, J.P.; Koshoffer, A.; Wickett, R.R.; Schwemberger, S.; Babcock, G.; Hakozaki, T.; Boissy, R.E. Epidermal keratinocytes from light vs. dark skin exhibit differential degradation of melanosomes. *J. Investig. Dermatol.* **2011**, *131*, 1226–1233. [CrossRef] [PubMed]
26. Zeng, H.; Harashima, A.; Kato, K.; Gu, L.; Motomura, Y.; Otsuka, R.; Maeda, K. Degradation of tyrosinase by melanosomal pH change and a new mechanism of whitening with propylparaben. *Cosmetics* **2017**, *4*, 43. [CrossRef]
27. Thong, H.Y.; Jee, S.H.; Sun, C.C.; Boissy, R.E. The patterns of melanosome distribution in keratinocytes of human skin as one determining factor of skin colour. *Br. J. Dermatol.* **2003**, *149*, 498–505. [CrossRef] [PubMed]
28. Chabot, B.; Stephenson, D.A.; Chapman, V.M.; Besmer, P.; Bernstein, A. The proto-oncogene c-kit encoding a transmembrane tyrosine kinase receptor maps to the mouse W locus. *Nature* **1988**, *335*, 88–89. [CrossRef] [PubMed]
29. Shimizu, Y.; Ashman, L.K.; Du, Z.; Schwartz, L.B. Internalization of Kit together with stem cell factor on human fetal liver-derived mast cells: New protein and RNA synthesis are required for reappearance of Kit. *J. Immunol.* **1996**, *156*, 3443–3449. [PubMed]
30. Grichnik, J.M.; Burch, J.A.; Burchette, J.; Shea, C.R. The SCF/KIT pathway plays a critical role in the control normal human melanocytes homeostasis. *J. Investig. Dermatol.* **1998**, *111*, 233–238. [CrossRef] [PubMed]
31. Peters, E.M.; Tobin, D.J.; Botchkareva, N.; Maurer, M.; Paus, R. Migration of melanoblasts into the developing murine hair follicle is accompanied by transient c-Kit expression. *J. Histochem. Cytochem.* **2002**, *50*, 751–766. [CrossRef] [PubMed]
32. Peters, E.M.; Maurer, M.; Botchkarev, V.A.; Jensen, K.D.; Welker, P.; Scot, G.A.; Paus, R. Kit is expressed by epithelial cells in vivo. *J. Investig. Dermatol.* **2003**, *121*, 976–984. [CrossRef] [PubMed]
33. Reber, L.; Da Silva, C.A.; Frossard, N. Stem cell factor and its receptor c-Kit as targets for inflammatory diseases. *Eur. J. Pharmacol.* **2006**, *533*, 327–340. [CrossRef] [PubMed]
34. Rönnstrand, L. Signal transduction via the stem cell factor receptor/c-Kit. *Cell. Mol. Life Sci.* **2004**, *61*, 2535–2548. [CrossRef] [PubMed]
35. Tsujimura, T.; Hashimoto, K.; Kitayama, H.; Ikeda, H.; Sugahara, H.; Matsumura, I.; Kaisho, T.; Terada, N.; Kitamura, Y.; Kanakura, Y. Activating mutation in the catalytic domain of c-kit elicits hematopoietic transformation by receptor self-association not at the ligand-induced dimerization site. *Blood* **1999**, *93*, 1319–1329. [PubMed]
36. Nishida, T.; Hirota, S.; Taniguchi, M.; Hashimoto, K.; Isozaki, K.; Nakamura, H.; Kanakura, Y.; Tanaka, T.; Takabayashi, A.; Matsuda, H.; et al. Familial gastrointestinal stromal tumours with germline mutation of the KIT gene. *Nat. Genet.* **1998**, *19*, 323–324. [CrossRef] [PubMed]
37. Isozaki, K.; Terris, B.; Belghiti, J.; Schiffmann, S.; Hirota, S.; Vanderwinden, J.M. Germline-activating mutation in the kinase domain of KIT gene in familial gastrointestinal stromal tumors. *Am. J. Pathol.* **2000**, *157*, 1581–1585. [CrossRef]
38. Beghini, A.; Tibiletti, M.G.; Roversi, G.; Chiaravalli, A.M.; Serio, G.; Capella, C.; Larizza, L. Germline mutation in the juxtamembrane domain of the kit gene in a family with gastrointestinal stromal tumors and urticaria pigmentosa. *Cancer* **2001**, *92*, 657–662. [CrossRef]
39. Hattori, H.; Kawashima, M.; Ichikawa, Y.; Imokawa, G. The epidermal stem cell factor is over-expressed in lentigo senilis: Implication for the mechanism of hyperpigmentation. *J. Investig. Dermatol.* **2004**, *122*, 1256–1265. [CrossRef] [PubMed]

40. Kunisada, T.; Lu, S.Z.; Yoshida, H.; Nishikawa, S.; Nishikawa, S.; Mizoguchi, M.; Hayashi, S.; Tyrrell, L.; Williams, D.A.; Wang, X.; et al. Murine cutaneous mastocytosis and epidermal melanocytosis induced by keratinocyte expression of transgenic stem cell factor. *J. Exp. Med.* **1998**, *187*, 1565–1573. [CrossRef] [PubMed]
41. Grichnik, J.M.; Crawford, J.; Jimenez, F.; Kurtzberg, J.; Buchanan, M.; Blackwell, S.; Clark, R.E.; Hitchcock, M.G. Human recombinant stem-cell factor induces melanocytic hyperplasia in susceptible patients. *J. Am. Acad. Dermatol.* **1995**, *33*, 577–583. [CrossRef]